Mahmood and Gul, J Material Sci Eng 2019, 8:3

Journal of Material Sciences & Engineering

Review Article **Open Access**

Conductivity, Structural and Thermal Studies on Electrospun PVA-PANI-$LiClO_4$-Sb_2O_3 Composite Nanofibers Polymer Electrolytes for Battery Applications

Wan Ahmad Kamil Mahmood and Rahmat Gul*

School of Chemical Sciences, Universiti Sains Malaysia, 11800 Minden, Pulau Penang, Malaysia

Abstract

Nanocomposite polymer blend electrolytes composed of poly(vinyl alcohol) (PVA) as a host polymer, Polyaniline (PANI) as an additive, Lithium Perchlorate ($LiClO_4$) as dopant salt were prepared for different concentrations of Antimony Trioxide (Sb_2O_3) as inorganic filler with the constant ratio of PVA and PANI polymers by using electrospinning technique and investigated. The complexations of the samples were analyzed using X-ray diffraction (XRD) and FTIR spectroscopic techniques which indicate complexation between the polymers, salt and inorganic filler whereas micro surface structure of the composite electrolytes was analyzed using scanning electron microscope (SEM) studies which reveal the surface morphology of the prepared samples. Thermogravimetric analyses (TGA) shows enhancement in thermal stability of composite polymer electrolytes films upon incorporation of filler. Sample films of PVA-PANI-$LiClO_4$-Sb_2O_3 were subjected to AC impedance spectroscopic analysis for the measurement of conductivity at different temperature. The effect of temperature and filler concentration on the ionic conductivity values have been studied in the range 298-353K. It was found that the polymer electrolyte with 9 wt% of Sb_2O_3 exhibits the highest ionic conductivity value of 8.394×10^{-5} S cm^{-1} at ambient temperature. The temperature dependence of the conductivity of the composite polymer electrolyte films seems to obey the VTF relation.

Keywords: Composite polymer electrolyte; AC impedance studies; X-ray diffraction analysis; Ionic conductivity; Antimony trioxide; FTIR; Poly(vinyl alcohol); Inorganic filler

Introduction

Recently, rapid development has been increased the demand for small size electronic devices which are possible only by miniaturizing the electrodes and electrolyte materials that are used in the batteries. Solid polymer electrolytes are of considerable interest for the last four decades, because of its importance and applications in many electrochemical devices such as Li-ion batteries, smart credit cards, super capacitors, cellular telephones, electro chromic devices, etc. [1,2]. The solid polymer electrolytes have many advantages compare to liquid electrolytes such as low costs, improved safety, ease of fabrication, and leakage free nature [3-6]. However, the main drawback their poor room temperature ionic conductivity restricts applications of solid electrolyte system in solid state batteries and electrochemical display devices. Several different methods of preparation have been carried out to improve the ambient temperature ionic conductivity, of various polymer electrolyte systems. The mechanical stability of most of the polymer electrolyte systems is greatly increased by using the process of polymer blending, rather than the single polymer electrolyte system. Among these systems, composite polymer electrolyte system provides majority of the requirements such as improved ionic conductivity, interfacial stability, mechanical stability and good thermal stability than other polymer electrolyte systems. The incorporation of inert phase inorganic metal oxide filler particles such as Al_2O_3, SiO_2, Fe_2O_3, ZrO_2, fly ash, etc to the host polymer materials has been reported to improve the ionic conductivity values. The addition of inorganic metal oxide particles is generally used to improve the ionic conductivity value of the polymer electrolyte systems [7-10]. The concentration and particle size of the inert phase metal oxide fillers has been found to greatly influence the enhancement in ionic conductivity. The increase in conductivity at ambient temperature is generally attributed either to the development of a new kinetic path, or to a concentration enhancement [11-14]. The incorporation of inert metal oxide filler into the polymer matrix greatly enhance the ionic motion though polymer electrolyte medium due to development of amorphous region [15,16]. Nanocomposite polymer electrolyte systems with polymer salt complex inorganic metal oxide are now being investigated [17].

In this study, the ambient temperature ionic conductivity and thermal stability of lithium ion hybrid polymer blend electrolyte films PVA-PANI-$LiClO_4$-Sb_2O_3 with various concentrations of Sb_2O_3 are examined which could give the highest ionic conductivity at room temperature. This has been achieved by adding a new type of inorganic nanofiller, Sb_2O_3, into polymer salt system. X-Ray diffraction (XRD), AC impedance spectroscopy, FTIR, thermogravimetric analysis (TGA), and scanning electron microscope (SEM) were carried out of the prepared nanocomposite polymer blend electrolyte systems for various concentrations of Sb_2O_3. The purpose of the present work is to study the effect of addition of Sb_2O_3 on the ionic conductivity of PVA-PANI-$LiClO_4$ polymer electrolyte systems.

Experimental Section

Materials

Poly(vinyl alcohol) (PVA) with an average molecular weight of 5×10^5 (Aldrich, USA), Polyaniline (PANI) with an average molecular weight of 10×10^5 (Aldrich, USA) and inorganic salt Lithium Perchlorate ($LiClO_4$) (E-Merck, Germany) were used without any

---

***Corresponding author:** Rahmat Gul, School of Chemical Sciences, Universiti Sains Malaysia, 11800 Minden, Pulau Penang, Malaysia, Tel: +6046533262; +6046533685; E-mail: rahmat388@yahoo.com

Received May 15, 2019; **Accepted** June 10, 2019; **Published** June 17, 2019

Citation: Mahmood WAK, Gul R (2019) Conductivity, Structural and Thermal Studies on Electrospun PVA-PANI-$LiClO_4$-Sb_2O_3 Composite Nanofibers Polymer Electrolytes for Battery Applications. J Material Sci Eng 8: 529.

further purification in the present study. All the reagents used to prepare polymer electrolyte complex membranes were analytical grade. PVA, PANI and $LiClO_4$ were vacuum dried before use, in the oven at 50°C, for 24 hours to remove moisture and other volatile impurities. All other reagents were commercially available and used as received for preparation of polymer electrolyte membranes in the electrospinning experiments.

Preparation of samples

Poly(vinyl alcohol) (PVA), Polyaniline (PANI) and Antimony Trioxide (Sb_2O_3) filler were used as the starting materials for the preparation of fibrous nanocomposite polymer electrolyte membranes by electrospinning technique. All the starting materials were dried at 50°C for 48 hours in hot air oven before use. Polymer solutions for electrospinning of PVA-Sb_2O_3 composite nanofiber polymer electrolyte membranes were prepared from 16 wt% poly(vinyl alcohol) (PVA) and polyaniline (PANI). For the development of fibrous nanocomposite polymer electrolyte membranes, 16 wt% of PVA and PANI polymer solutions were prepared by dissolving the required amounts of PVA and PANI in distilled water homogeneously under continuous magnetic stirring for 6 h at room temperature and degassed to remove air bubbles. Later, 4, 8, 12, 16 and 20 wt% of Sb_2O_3 nanoparticle filler were added to the above optimized 16 wt% PVA polymer solution under constant stirring of the ingredients for 6 hours to obtain a homogeneous and transparent polymer solution containing Sb_2O_3 of concentration varying in the range 4-20 wt% and then cooled to room temperature. The concentrations of Sb_2O_3 in the composite polymer solutions were based on the weight of PVA and PANI. The resulting polymer solutions were degassed to remove air bubbles. The resultant viscous polymer solutions were electrospun to prepare the membranes. The polymer solution was held in a 3 ml syringe and loaded in a syringe withdrawal pump (New Era Pump Systems Inc., model NE-300) to prepare electrospun nanocomposite fiber polymer electrolyte membranes by electrospinning technique after setting the essential electrospinning parameters. The electrospinning was carried out at room temperature and below 40% RH, a high positive voltage of 20 kV to the composite solutions between spinneret and collector was applied by using a high voltage power supply (Spellman, model CZE1000R) which could generate positive DC voltages up to 30 kV, and distance between the tip of the spinneret and grounded stainless steel plate collector covered with thin aluminum foil was 10 cm, needle bore size 24 G, and the filler concentrations in the blend polymer solution were 4, 8, 12, 16, and 20 wt%. The steel needle was connected to an electrode of a high positive voltage supply and the composite polymer solution held in a 3 ml syringe was delivered into a needle spinneret by a syringe withdrawal pump (Spellman, model CZE1000R) with a flow rate of 2 ml h^{-1}. The electrospun fibrous nanocomposite polymer electrolyte membranes were collected on a grounded stainless steel plate covered with thin aluminum foil and dried under vacuum in oven at 50°C for 48 hours to remove the solvent before further use. All experiments were carried out at room temperature and below 25% environmental humidity. After electrospinning, each of the obtained nanofiber membranes were carefully peeled off from the stainless steel plate covered by thin aluminum foil and placed in a vacuum oven under 50°C for 24 hours to remove any remaining solvent and then stored in a glove box.

Characterization

The prepared electrolytes were subjected to AC impedance analysis, in order to calculate the ionic conductivity. This ionic conductivity of the samples was measured by steel blocking electrodes in the frequency range 1 Hz-100 kHz at various temperatures using HIOKI 3532-50 LCR Hi-tester. The films were sandwiched between two stainless ranging from 298 to 353K. The XRD patterns were recorded with the XRD equipment Siemens D 5000 diffractometer with Cu-Kα radiation as source, over the range of $2\theta=5-80°$ at ambient temperature and operated at 40 kV. The sample was scanned in the 2θ ranging from 10 to 80° for 2 s in the step scan mode. The Fourier transform infrared spectra (FTIR) were recorded using a Perkin Elmer Paragon Model 500 spectrophotometer in the 4000-400 cm^{-1} region. The thermal analysis (TGA) of the sample was carried out using Perkin Elmer TG/DTA (Pyris Diamond thermo gravimetric analyzer) with the heating rate of 10°C min^{-1} between 30°C and 400°C in nitrogen gas atmosphere. Surface morphology of the composite polymer electrolyte samples was recorded by means by using JEOL, JSM-840A scanning electron microscope (SEM) model and examined at 10 kV at room temperature

Results and Discussion

Conductivity studies

The effect of incorporation of inorganic filler Sb_2O_3 to the polymer electrolyte complexes on its ionic conductivity value has been studied. Figure 1 shows the Arrhenius plot of the variation of ionic conductivity as a function of different wt% of Sb_2O_3 filler concentration of the prepared PVA-PANI blend polymer electrolyte systems over the temperature range 298-353K. The estimated ionic conductivity values are given in Table 1. The conductivity values for nanocomposite polymer electrolyte PVA-PANI-$LiClO_4$ shows that conductivity increases with addition of Sb_2O_3 filler. It is found from Table 1 that ionic conductivity of polymer electrolyte systems with different filler concentration are in the range from 1.51×10^{-9} to 8.394×10^{-5} S cm^{-1} at 298 K. It is the Table 1 that the ionic conductivity value increases with the concentration of Sb_2O_3 filler until an optimum concentration is reached, and shows a maximum value of 8.394×10^{-5} S cm^{-1} at room temperature corresponding to the polymer electrolyte systems with a 9 wt% of filler afterwards it is found to retard with further addition. It is found that the conductivity decreases with Sb_2O_3 content in the region of high Sb_2O_3 concentration (15 wt%) in the polymer complex. A maximum ionic conductivity is evaluated for the sample containing 9 wt% of Sb_2O_3 at all studied temperatures. The maximum room temperature ionic conductivity value 8.394×10^{-5} S cm^{-1} is obtained for the sample with 9 wt% Sb_2O_3. The initial rise in conductivity (Figure 2) at low filler contents, Sb_2O_3

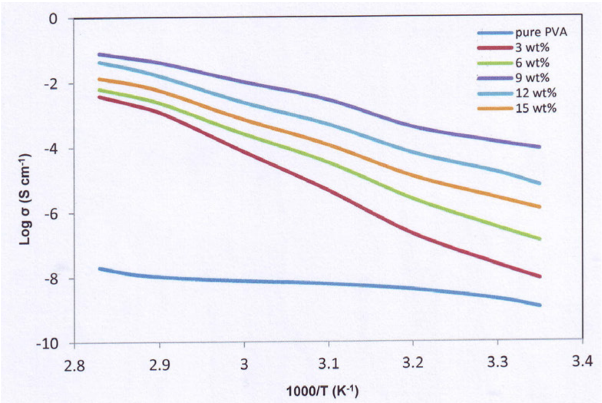

Figure 1: Arrhenius plot of log conductivity against reciprocal temperature of PVA-PANI-$LiClO_4$-Sb_2O_3 polymer complexes with different concentrations of $LiClO_4$ salt.

Composition of PVA-PANI-$LiClO_4$-Sb_2O_3 wt%	**Ionic conductivity values (σ) Scm^{-1} at different temperatures**							
	298 K	**303 K**	**313 K**	**323 K**	**333 K**	**343 K**	**348 K**	**353 K**
Pure PVA	1.12×10^{-9}	1.99×10^{-9}	3.98×10^{-9}	6.02×10^{-9}	7.58×10^{-9}	1×10^{-8}	1.25×10^{-8}	1.99×10^{-8}
PVA-PANI-$LiClO_4$-Sb_2O_3 (60-30-10^{-3})	1.51×10^{-9}	2.29×10^{-8}	2.04×10^{-7}	4.45×10^{-6}	7.16×10^{-5}	9.54×10^{-4}	2.06×10^{-3}	3.8×10^{-3}
PVA-PANI-$LiClO_4$-Sb_2O_3 (60-30-10^{-6})	1.23×10^{-7}	3.1×10^{-7}	2.39×10^{-6}	3.26×10^{-5}	2.54×10^{-4}	1.94×10^{-3}	3.80×10^{-3}	6.30×10^{-3}
PVA-PANI-$LiClO_4$-Sb_2O_3 (60-30-10^{-9})	8.39×10^{-5}	1.33×10^{-4}	4.07×10^{-4}	2.81×10^{-3}	1×10^{-2}	3.6×10^{-2}	5×10^{-2}	7×10^{-2}
PVA-PANI-$LiClO_4$-Sb_2O_3(60-30-10^{-12})	6.30×10^{-6}	1.58×10^{-5}	6.38×10^{-5}	4.94×10^{-4}	2.39×10^{-3}	1.3×10^{-2}	2×10^{-2}	4×10^{-2}
PVA-PANI-$LiClO_4$-Sb_2O_3(60-30-10^{-15})	1.17×10^{-6}	2.51×10^{-6}	1.18×10^{-5}	1.13×10^{-4}	7.07×10^{-4}	4.6×10^{-3}	8.91×10^{-3}	1×10^{-2}

Table 1: Temperature dependent ionic conductivity values of the prepared complexes.

would contribute to dissociation of lithium salt, which leads to the availability of charge carrier up to the optimum concentration (9 wt% of filler) supplied by the PVA-PANI-$LiClO_4$-Sb_2O_3 polymer complexes resulting in enhancement of total ionic conductivity. The highest value in ionic conductivity vs. polymer electrolyte composition behaviour observed in Figure 2 may be attributed to decrease in crystallinity of the polymer electrolyte systems. But continuous non-conductive phase develops at high contents of electrically inert metal oxide filler would block up transportation of ions, which may cause increase in the total resistance of the polymer electrolyte systems [18]. The Lewis acid groups of the added inert filler in the polymer electrolyte samples compete with the Lewis acid lithium cations for complexation with polymer chains and the anions of the added salt [19]. The Lewis acid base interaction centers interact with the electrolytes, and increases salt dissociation by ion-filler complexation and lowering the ionic coupling.

The temperature dependent ionic conductivity plot of the prepared nanocomposite polymer blend electrolyte systems are shown in Figure 1. It has been noted that as the temperature increases, the ionic conductivity value also increase for all the complexes irrespective of compositions because as the temperature increases, the vibrational energy of the polymer segment also increases, and the polymer can expand easily creating a small amount of free volume through which the ionic motion occurs. Thus ions solvated molecules or polymer segments can move into the free space or free volume. The resulting ionic conductivity is represented by the available free volume around the polymer chains. The increase in free volume causes increase in ionic and segmental mobility of the polymer electrolyte systems. In addition to that the availability of free volume also reduces the retarding effect of ionic clouds which lead to higher ionic conductivity at higher temperatures. The overall features of the Arrhenius plot are quite similar for the polymer electrolyte systems and the temperature dependence of the ionic conductivity is non-linear in this plot which indicates that the ionic conduction seems to fits well with the Williams-Landel-Ferry (WLF) mechanism [20] which describes the transport properties in a viscous matrix [21-23]. The non-linearity of plot indicates that transportation of ions in polymer electrolyte systems is dependent on segmental motion of polymers [24]. Therefore, the observed result may be more effectively represented by the empirical Vogel-Tamman-Fulcher (VTF) relation:

$$\sigma = A T^{-1/2} \exp[-B/T\text{-}Tg],$$

where A and B are constants and Tg the reference temperature taken as the glass transition temperature. Constant A in VTF equation is related to the number of charge carriers in the polymer electrolyte system and constant B is related to the activation energy of transportation of ions.

XRD analysis

The X-ray diffraction analysis is a useful tool for the structural elucidation and crystallization of the polymer electrolytes. X-ray diffraction measurements were performed to investigate the effect of Sb_2O_3 concentration (3, 6, 9, 12 and 15 wt%) on the structural properties of the PVA based complexed nanocomposite polymer electrolyte PVA-PANI-$LiClO_4$-Sb_2O_3 systems. The XRD patterns of pristine PVA, PANI, Sb_2O_3, $LiClO_4$ and the complexes are shown in Figure 3a, 3b, 3h, 3i and 3c-3g, respectively. XRD diffractogram of Sb_2O_3 and $LiClO_4$ reveals the high crystalline nature of the inorganic filler Sb2O3 and the LiClO4 salt. The crystalline diffraction peaks for Sb_2O_3 at angles of 2θ=28.5°, 41.3°, 44.7°, 50.7°, 55.7°, 58.7° and 66.6° are shown in Figure 3h. The sharp crystalline peaks for LiClO4 salt observed at angles of 2θ=23.1°, 27°, 31°, 33.6°, 36.2° and 39.4° as depicted in Figure 3a confirms the complete crystalline nature of $LiClO_4$ salt. The presence of broad hump (Figure 3a) indicates the amorphous nature of the PVA polymer. The characteristic crystalline peak of PVA observed at angles of 2θ=19.23° elucidates the partial crystalline nature of PVA which gives an overall semi-crystalline morphology for PVA Figure 3a. It has been observed that the addition of $LiClO_4$ salt and Sb_2O_3 filler disturbed the arrangement in the polymer backbone of PVA resulting decreased crystallinity and increased amorphicity of PVA and hence intensity of the crystalline peak is reduced. Figure 3a indicates that the intensity of the crystalline diffraction peaks of PVA at 2θ=19.23° decreases and broadens by increasing the Sb_2O_3 content (Figure 3c-3d) up to certain level, above this optimum value of concentration, the intensity of the characteristic diffraction peaks increases with the increase of filler content in the matrix Figure 3e-3g. Such reduction in crystallinity may be attributed to the changes in the reorganization of polymer chain upon the addition of small particles of inorganic inert fillers which facilitates for higher ionic conductivity [25]. Results show that the relative peak at 2θ=19.23° for pure PVA had shifted to 2θ=16.2°, 19.87°, 16.72°, 16.8° and 19.17° in the polymer electrolyte systems containing 3, 6, 9, 12 and 15 wt% Sb_2O_3, respectively. The shifting of peaks is attributed to the addition of $LiClO_4$ salt and Sb_2O_3 filler. This phenomenon shows

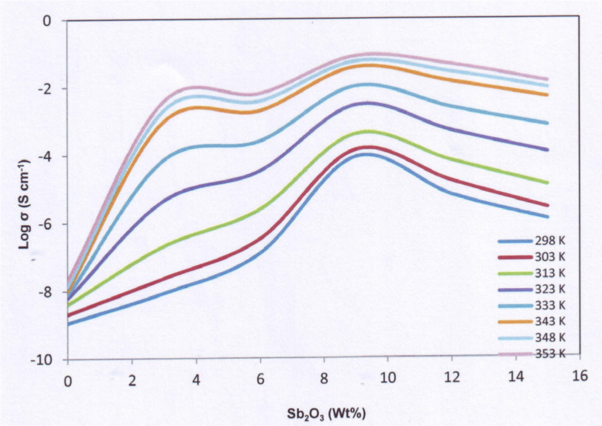

Figure 2: Plot of log conductivity vs. composition of PVA-PANI-$LiClO_4$-Sb_2O_3 at various temperatures.

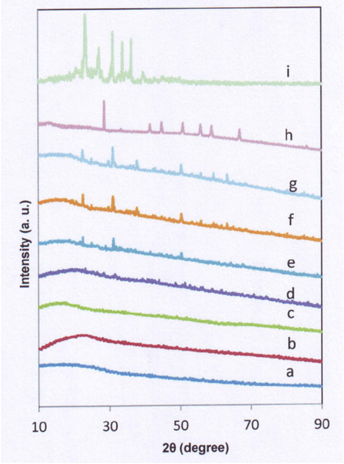

Figure 3: X-ray diffraction spectrum of (a) pure PVA (b) pure PANI (c) PVA-PANI-$LiClO_4$-Sb_2O_3 (60-30-10-3) (d) PVA-PANI-$LiClO_4$-Sb_2O_3 (60-30-10-6) (e) PVA-PANI-$LiClO_4$-Sb_2O_3 (60-30-10-9) (f) PVA-PANI-$LiClO_4$-Sb_2O_3 (60-30-10-12) (g) PVA-PANI-$LiClO_4$-Sb_2O_3 (60-30-10-15) (h) pure Sb_2O_3 (i) pure $LiClO_4$.

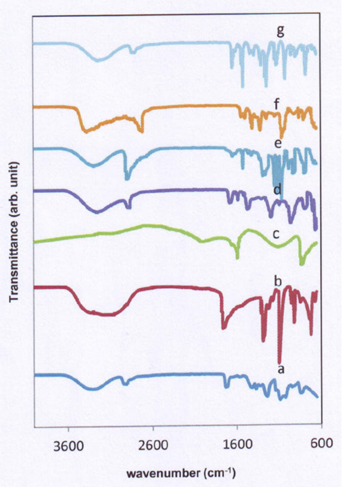

Figure 4: FTIR spectrum of (a) Pure PVA, (b) Pure PANI (c)$LiClo_4$ salt and PVA-PANI-$LiClO_4$ (60-30-10) complex solid polymer electrolyte systems with (d) 3 wt% Sb_2O_3 (e) 6 wt% Sb_2O_3 (f) 9 wt% Sb_2O_3 (g) 12 wt% Sb_2O_3.

that complex formation has occurred between PVA, $LiClO_4$ and Sb_2O_3. The relative diffraction peak intensity of PVA corresponding to 9 wt% of the filler appears broader and becomes lightly less prominent with further addition of Sb_2O_3 revealing that the amorphous nature of the complex polymer electrolyte is enhanced which is responsible for higher polymer chain flexibility as well as ionic conductivity. The sharp crystalline peaks (27°, 33.7° and 36.2°) pertaining to $LiClO_4$ (Figure 3i) and sharp crystalline peaks (28.5°, 41.5°, 44.8°, 56° and 66.9°) pertaining to Sb_2O_3 (Figure 3h) were found to be disappear in the complexes, indicating the complete dissolution of lithium salts and inorganic filler in the polymer complexes. These observations suggest that the polymer undergoes significant structural modifications. Few crystalline peaks were reappeared from the XRD diffractogram of Sb_2O_3 (31°, 50.8°, 58.9°) in the polymer electrolyte complexes. This may be attributed to excess amount of Sb_2O_3 that does not undergo complexation with the PVA-$LiClO_4$ matrix. It is observed from the Figure 3c-3g that the characteristic diffraction peaks pertaining to the lithium salts (23.1°, 36.2°, 39.4°) and Sb_2O_3 filler are mislaid in the complexes indicates the absolute dissolution of the salt in the polymer matrix [26]. Results also indicate that addition of Sb_2O_3 filler decreases the intensity of crystalline diffraction peaks which pertaining to $LiClO_4$ salt. The effect of Sb_2O_3 filler shows that lithium salt dissociates into free ions upon the addition of filler, which is in good agreement with ionic conductivity studies. Addition of Sb_2O_3 had increased the amorphicity of the polymer electrolyte systems. The polymer electrolyte system with 9 wt% filler which gives the maximum ionic conductivity has the lowest crystallinity. The crystallinity was increased with further incorporation of Sb_2O_3 filler due to excessive amount of filler content. This is attributed to the formation of aggregates. Few characteristic diffraction peaks (3.1°, 36.2°, 39.4°) pertaining to the Li salt are shifted from its position.

FTIR analysis

Infrared spectral analysis monitors the vibrational energy levels in the region of different molecules. The FTIR spectra for PVA, PMMA, $LiClO_4$, Sb_2O_3 and the polymer complexes, are shown in Figure 4a-4g, respectively. The free O-H stretching vibration frequency band in the FTIR spectrum is the most characteristic feature of alcohols and phenols, and occurs at 3433 cm^{-1} in pure PVA. The hydroxyl vibrational frequency band in the polymer electrolyte complexes is shifted towards the lower wave numbers, and it confirms the occurrence of specific interactions in the polymer matrices. The broad hydroxyl frequency band is shifted towards lower wave numbers 3295, 3300, 3384 and 3250 cm^{-1} in the polymer complexes containing 3, 6, 9 and 12 wt% Sb_2O_3 respectively due to hydrogen bond formation. This gives a clear indication of complexation in the polymer matrices. The characteristic vibrational frequency band appears at 2942 cm^{-1} is corresponding to asymmetric CH_2 stretching vibration in pure PVA and is displaced to 2865, 2896, 2712, and 2819 cm^{-1} in the complexes containing 3, 6, 9 and 12 wt% Sb_2O_3 respectively. The vibrational peak at 1433 cm^{-1} is assigned to a CH_2 scissor mode of pure PVA and is displaced to 1480, 1293, 1312, and 1241 cm^{-1} in the complexes containing 3, 6, 9 and 12 wt% Sb_2O_3 respectively.

The peak at 1729 cm^{-1} pertaining to C=O stretching of unhydrolyzed acetate group of PVA, and is displaced towards lower wave numbers 1688, 1654, 1543 and 1646 cm^{-1} in the complexes containing 3, 6, 9 and 12 wt% Sb_2O_3 respectively. The characteristic vibrational frequency band at 1097 cm^{-1} is corresponding to C-O stretching of secondary alcohols, and is displaced to 960, 920, 806, and 779 cm^{-1} in the complexes containing 3, 6, 9 and 12 wt% Sb_2O_3 respectively.

Thermo gravimetric analysis TGA analysis

Thermo gravimetric analysis technique has been widely used to study the physical changes encountered by the polymer electrolyte systems during thermal excitation which gives a rough idea of the kind of changes the polymer electrolyte may undergo in the working atmosphere. The process involves change in weight attributed to moisture uptake and thermal stability of the polymer electrolyte system. In the present work, TGA trace was recorded in order to examine the thermal stability of the polymer electrolyte samples. Figure 5a-5e illustrates the Typical TGA thermogram of the sample PVA, and polymer electrolyte films containing constant PVA-PANI ratio (60-30) with various concentrations of filler. From the themograph, it is observed that the sample is thermally stable up to 330°C. The TGA of PVA film shows two major weight loss regions. There is a gradual weight loss until the sample reaches 110°C in the temperature range 100-110°C for the pure PVA, and other polymer

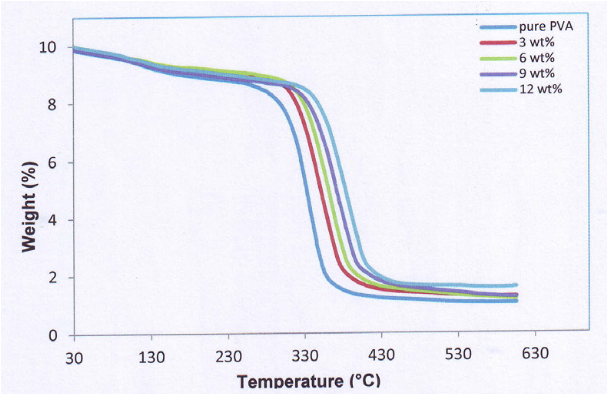

Figure 5: TG curves of (a) pure PVA (b) PVA-PANI-$LiClO_4$-Sb_2O_3 (60-30-10-3) (c) PVA-PANI-$LiClO_4$-Sb_2O_3 (60-30-10-16) (d) PVA-PANI-$LiClO_4$-Sb_2O_3 (60-30-10-9) (e) PVA-PANI-$LiClO_4$-Sb_2O_3 (60-30-10-12).

electrolyte films irrespective of the filler concentration which could be due to the elimination of the residual solvent and the evaporation of weakly physical bound moisture or removal of impurities absorbed while loading the sample [27]. The second weight loss occurring at around 270°C is due to the decomposition of PVA film. In addition, the weight loss of PVA also increases as the temperature increases from 280°C to 350°C. This might be attributed to the carbonation [28]. Polymer electrolytes with different concentrations of Sb_2O_3 also show two stages of weight loss. First stage of the weight loss is attributed to the evaporation of free and bound water. Figure 5 also shows that there is a second weight loss for nanocomposite polymer electrolytes at the temperature range of 310-330°C. The films having 3, 6, 9 and 12 wt% of filler is found to be stable up to 310, 315, 325 and 330°C with gradual weight loss. The decomposition temperature has shifted towards higher temperature upon the addition of $LiClO_4$ and Sb_2O_3. The decomposition temperature of films with 0 wt% of filler is found to be approximately 270°C whereas decomposition temperature of nanocomposite polymer electrolyte systems with fillers is approximately 330°C. The addition of Sb_2O_3 has enhanced the thermal stability of the nanocomposite polymer electrolyte membranes where polymer membranes with filler undergo decomposition at higher temperature. The remaining residue around 20 wt% may be due to the presence of inorganic filler Sb_2O_3. Results show that the incorporation of inorganic filler Sb_2O_3 to the polymer electrolyte systems had reduced the percentage of weight loss. It is concluded that the thermal stability of the polymer electrolyte systems increased effectively upon the addition of inorganic filler Sb_2O_3. These polymer electrolyte systems have become more thermally stable and more resistant to heat as compared to composite polymer electrolyte systems without inorganic filler. Even though the polymer electrolyte with 9 wt% of salt is found to have a thermal stability lower than the other films, this film is considered to be the best film on the basis of conductivity.

Scanning electron microscopy (SEM)

Figure 6a and 6b depicts the SEM micrograph images of electrospun nanofiber pure PVA and PVA-PANI-$LiClO_4$-Sb_2O_3 (60-30-10-9) composite solid polymer electrolyte membrane with 9 wt% concentration of Sb_2O_3 filler. The observed SEM images of the electrospun nanofiber membranes reveal the presence of fully well interconnected closed pores between the fibers of the samples made up of polymeric chains. It can be seen from the SEM images that electrospun membranes which formed by the interconnected ultrafine fibers in the sub micrometer range, generates three dimensional network structure with a random fiber orientation and high porosity. This unique porous structure formed by interlaying of fibers in the form of stacked layers facilitates an electrolyte to diffuse smoothly and it is beneficial to entrap and retain electrolyte. SEM of pure PVA films shows no features attributed to any crystalline morphology. From the figure, it is obvious that the morphology of these nanofiber polymer electrolyte membrane is uniform type but with different degrees of roughness. It can be seen that surface morphology of the PVA-PANI-$LiClO_4$-Sb_2O_3 system exhibit filler aggregates on the top surface of the polymer membrane. The surface morphology of the composite nanofiber membrane become rough compare with the pure PVA membrane. But as a whole it can be observed that Sb_2O_3 filler is homogeneously distributed in the polymer matrix which indicates uniform and homogeneous compatibility of PVA polymer matrix with Sb_2O_3 filler.

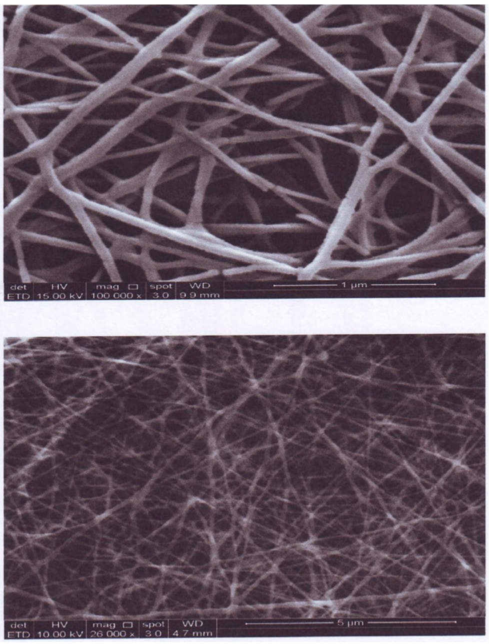

Figure 6: SEM images of (a) Pure PVA (b) PVA-PANI-$LiClO_4$-Sb_2O_3 (60-30-10-9).

The surface morphology of the electrospun nanofiber membrane also depends on the composition of solvent. The amount of residual solvent molecules on the membrane after electrospinning may partially dissolve the membrane and make the sample amorphous. The solvent molecules on the surface of membrane can also cause physical crosslink between the fibers of membranes.

Conclusions

Nanocomposite polymer electrolyte systems based on the blend of PVA-PANI with constant concentration of $LiClO_4$ salt were prepared for various concentrations of Sb_2O_3 filler. Conductivity increases and then decreases with the addition of Sb_2O_3. It was found that the PVA-PANI-$LiClO_4$-Sb_2O_3 polymer electrolyte system with a 9 wt% of Sb_2O_3 filler exhibits the highest value of ionic conductivity of the order 8.394×10^{-5} S cm^{-1} than the other concentrations at room temperature. TGA analyses also shows that the incorporation of Sb_2O_3 improves the thermal stability of the nanocomposite polymer electrolyte complexes and the sample having highest ionic conductivity with 9 wt% of Sb$_2$O$_3$ is thermally stable up to 385°C. X-ray diffraction analysis have confirmed that the incorporation of Sb$_2$O$_3$ filler improve the amorphous characteristic as well as the ionic conductivity of polymer electrolyte systems by the dissolution of the lithium salt and the interaction between the Sb$_2$O$_3$ filler and the polymer salt complex. The complexation in PVA-PANI-LiClO$_4$-Sb$_2$O$_3$ polymer electrolyte system has been confirmed from FTIR studies. SEM images revealed the morphological studies showing the complex formation between Sb$_2$O$_3$ and polymer electrolyte systems. This optimized polymer electrolyte system for possible high energy density batteries fabrication shows good ionic conductivity and thermal stability.

Acknowledgment

The authors gratefully acknowledge the financial support of the School of Chemical Sciences, USM (Malaysia) and TWAS, in the form of a research project, to carry out the research work. One of the authors (Rahmat Gul) acknowledges the University Sains Malaysia (USM), Penang, Malaysia and TWAS, for the award of Post-Doctoral Fellowship.

References

1. Aihara Y, Kodama M, Nakahara K, Okise H, Marata K (1997) Characteristics of a thin film lithium-ion battery using plasticized solid polymer electrolyte. J Power Sources 65: 143-147.
2. Armand M (1994) The history of polymer electrolytes. Solid State Ionics 69: 309-319.
3. Angulakshmi N, Sabu Thomas KS, Nahm A, Manuel Stephan R, Nimma E (2011) Electrochemical and mechanical properties of nanochitin-incorporated PVDF-HFP-based polymer electrolytes for lithium batteries. Ionics 17: 407-414.
4. Manuel Stephan A (2006) Review on gel polymer electrolytes for lithium batteries. Eur Polym J 42: 21-42.
5. Mc Callum JR, Vincent CA (1987) Polymer Electrolytes Reviews Elsevier, London.
6. Manuel Stephan A, Nahm KS (2006) Review on composite polymer electrolytes for lithium batteries. Polymer 47: 5952-5964.
7. Kelly J, Owen JR, Steele BCH (1984) Mixed polyether lithium-ion conductors. J Electroanal Chem 168: 467-478.
8. Kelly J, Owen JR, Steele BCH (1985) Poly (ethylene oxide) electrolytes for operation at near room temperature. J Power Sources 14: 13-21.
9. Ito Y, Kanehori K, Miyauchi K, Kudo TJ (1987) Mater Sci 22: 1845
10. Przyluski J, Wieczorek W (1989) Increasing the conductivity of polymer solid electrolytes: A review. Solid State Ionics 36: 165-169.
11. Liang CC (1973) Conduction characteristics of the lithium iodide-aluminum oxide solid electrolytes. J Electrochem Soc 120: 1289-1292.
12. Mac Callum JR, Vincent CA (1987) Polymer electrolyte reviews. (1stedn), Elsevier Applied Science Publishers, London.
13. Maier J (1989) Superionic solids and solid electrolytes. (1stedn), Academic Press.
14. Wagner JB (1989) High conductivity solid ionic conductors. (edited by Takahashi T), Singapore: World Scientific.
15. Ahn JH, Wang GX, Liu HK, Dou SX (2003) Nanoparticle-dispersed PEO polymer electrolytes for Li batteries. J Power Sources 422: 119-121.
16. Sun HY, Takeda Y, Imanishi N, Yamamoto O, Sohn HJ (2000) Ferroelectric materials as a ceramic filler in solid composite polyethylene Oxide-Based electrolytes. J Electrochem Soc 147: 2462-2467.
17. Wieczorek W, Such K, Wycislik H, Plocharski J (1989) Modifications of crystalline structure of PEO polymer electrolytes with ceramic additives. Solid State Ionics 36: 255-257.
18. Itoh T, Ichikawa Y, Uno T, Kubo M, Yamamoto O (2003) Composite polymer electrolytes based on poly (ethylene oxide), hyperbranched polymer, BaTiO3 and LiN (CF3SO2) 2. Solid State Ionics 156: 393-399.
19. Croce F, Persi L, Scrosati B, Fiory FS, Plichta E, et al. (2001) Role of the ceramic fillers in enhancing the transport properties of composite polymer electrolytes. Electrochim Acta 46: 2457-2461.
20. Williams ML, Landell RF, Ferry JD (1955) The temperature dependence of relaxation mechanisms in amorphous polymers and other glass-forming liquids. J Am Chem Soc 77: 3701-3707.
21. Vogel H (1922) Das temperaturabhängigkeitsgesetz der viskosität von flüssigkeiten. Phys Z 22: 645-646.
22. Tamman VG, Hesse HZ, Allg A (1926) Chem 19: 245.
23. Fulcher GJ (1925) Analysis of recent measurements of the viscosity of glasses. Am Ceram Soc 8: 339-355.
24. Okamoto V, Yeh TF, Lee HS, Skotheimic TA (1993) Design of alkaline metal ion conducting polymer electrolytes. J Polym Sci Part A: Polymer Chemistry 31: 2573-2581.
25. Wieczorek W, Steven JR, Florjanczyk Z (1996) Composite polyether based solid electrolytes. The Lewis acid-base approach. Solid State Ionics 85: 67-72.
26. Jacob MME, Prabaharan SRS, Radhakrishna S (1997) Effect of PEO addition on the electrolytic and thermal properties of PVDF-LiClO4 polymer electrolytes. Solid State Ionics 104: 267-276.
27. Rajendran S, Ravi SB, Sivakumar P (2007) Effect of salt concentration on poly (vinyl chloride)/poly (acrylonitrile) based hybrid polymer electrolytes. Journal of Power Sources 170: 460-464.
28. Ganesan S, Muthuraaman B, Mathew V, Madhavan J, Marumuthu P, et al. (2008) Reporting solar cell efficiencies in Solar Energy Materials and Solar Cells. Solar Energy Materials and Solar Cells 92: 371-373.